HiSST: 3rd International Conference on
High-Speed Vehicle Science Technology
14 -19 April 2024, Busan, Korea

Preliminary Study of High-Speed Variable Geometry Two-Dimensional Inlet Design

Jun Liu[1], Xueju Qiu[2],Huacheng Yuan[3]

Abstract

In order to meet the thrust and mass flow requirements of the new concept aero-engine within the altitude range of 0-30 km and the Mach number range of 0-5, this paper proposes a new external compression method which consists of isotropic compression and ramp compression. Firstly, the inlet capture area is set as 2.0 m^2 based on the engine airflow requirements, and the inlet aerodynamic schemes are designed at different design points (Ma2.5, Ma3.6, Ma5.0). The results indicate that inlet aerodynamic scheme for the design point Ma3.6 is the best. Secondly, the variable geometry scheme of the two-dimensional inlet within the Ma 0-5 range is studied. In order to improve the total pressure recovery coefficient of the inlet, the throat Mach number of the inlet is controlled within the range of Ma1.2-Ma1.5. The total pressure recovery coefficient of the design point inlet is 0.96 at throat section. The maximum total pressure recovery at aerodynamic interface plane reaches 0.70, which is 5.9% higher than the requirement. Finally, the velocity characteristics of the variable geometry inlet are studied. The operation range of the inlet is widen through adjusting the angle of the second compression ramp and the shoulder boundary layer suction. The results indicate that the inlet meets the requirement of aero-engine at a wide range.

Keywords: *two-dimensional inlet, variable geometry, wide Mach number range*

Nomenclature (Tahoma 11 pt, bold)

Latin
A – Area
ICR – Internal compression ratio
Ma – Mach number
P* – Total pressure
T* – Total temperature
Ls – diffuser length
Ys – diffuser offset
h – Altitude
m – mass flow rate
Greek
β – shock angle
δ – ramp deflection angle
φ– mass flow ratio
σ– Total pressure recovery coefficient
Superscripts
H – A superscript
Subscripts
0 – far-field section
t – throat section
c – inlet capture section

1. Introduction

As one of the important components of an air-breathing propulsion system, the inlet plays a critical role in providing the uniform airflow for the aero-engine [1-3]. For conventional fixed-geometry inlets, there is a significant drop in the mass flow coefficient at the off-design points, and there is a large separation

[1] *Nanjing University of Aeronautics and Astronautics, Yudao Street 29#, Nanjing City, Jiangsu Province, China, E-mail liujunnever@nuaa.edu.cn*
[2] *Nanjing University of Aeronautics and Astronautics, Yudao Street 29#, Nanjing City, Jiangsu Province, China, E-mail 161172791@qq.com*
[3] *Nanjing University of Aeronautics and Astronautics, Yudao Street 29#, Nanjing City, Jiangsu Province, China, E-mail yuan_public@126.com*

result in total pressure loss. The aerodynamic performance is poor at off-design points[4]. Therefore, fixed-geometry inlets cannot meet the requirements of a wide Mach number and altitude range for aircraft engines. In this case, variable geometry inlets have attracted widespread attention and research from scholars all around the world due to their good inlet flow matching within a wide speed range and advantages such as low Mach number self-starting. Among the different types of inlet, the two-dimensional inlet, with its simple variable geometry structure and easy integration with the aircraft design, has been widely used in the field of variable geometry inlets. Typical examples include the HYPR engine two-dimensional inlet, the Scimitar engine two-dimensional inlet, and the two-dimensional inlet developed by TechLand Research [5].

The two-dimensional inlet is currently widely used and research. Wang [6] proposed a freely-shaped two-dimensional inlet design method, and conducted a parametric study on the two-dimensional inlet. The aerodynamic performance requirements for a wide range of Mach 2.5-8 were successfully achieved without the need for design points. Zhu et al. used a reverse design method for the internally and externally compressible curved compression inlet with controllable surfaces[7]. They designed a new two-dimensional curved compression inlet and obtained wide Mach number range performance. They achieved a high total pressure recovery coefficient within the Mach number range of 2-4 at 3° angle of attack. The two-dimensional variable geometry inlet with a Mach range of 0-6 was used in the Japanese JAXA Turbojet and Ramjet Combined Cycle (TBCC) engine[8]. They controls the throat Mach number around 1.5 by adjusting the second ramp compression angle, ensuring high performance throughout the operating range. Sanders et al. designed an over/under two-dimensional inlet for TBCC engines in the Mach range of 0-7[9]. The compression ramp angle and lip angles are adjusted through a variable geometry adjustment mechanism to achieve mode transition and ensure a good aerodynamic performance.

To improve the starting ability of the inlet within a wide range Mach number, boundary layer bleeding is an effective method[10]. Yuan et al. [11] investigated a supersonic two-dimensional inlet with different bleeding ratios and found that boundary layer bleeding can effectively reduce the starting Mach number of the inlet. Chen et al.[12] studied the layout and bleeding slot angles effect on the total pressure recovery coefficient, bleeding mass flow rate ratio, and throat pressure ratio. They found that at the same bleeding area, total pressure recovery coefficient increases with the number of bleeding slots.

This paper aims to design a two-dimensional inlet to meet the requirements of wide Mach number range aeroengine. Firstly, the mass flow requirement of the wide Mach number range aeroengine are listed. Then a baseline variable geometry two-dimensional inlet was design according to the flow requirement of the aeroengine. Finally, the flow characteristics and properties of the inlet at different inflow condition and engine operation conditions are discussed.

2. Two-dimensional inlet geometry

2.1. Inlet requirement

The main inlet capture mass flow and total pressure recovery requirements are shown in Table 1. The aero-engine operates from sea-level static to Mach number 5.0 at altitude 30km. It operates in turbofan mode until Mach number 4.0. The mode transition from turbofan mode to turbojet mode between Mach number 3.6 and 4.0. Then it operates in turbojet mode until Mach number 5.0.

Table 1. Inlet requirement

	H	Ma	m(kg/s)	σ	P_0^*（kPa）	T_0^* (K)	m_{cor}(kg/s)
Turbofan mode	0	0	124.23	0.97	101325	288.15	128.07
	11	0.8	46.26	0.97	22700	216.77	128.97
	11	1.3	75.27	0.9529	22700	216.77	128.02
	11	1.5	94.56	0.9415	22700	216.77	127.90
	20	2.4	64.83	0.8601	5529	216.65	128.92
	20	2.5	70.22	0.8422	5529	216.65	116.19
	23	3.2	68.44	0.7427	3467	219.56	79.38
	26	3.6	57.81	0.664	2188	222.54	69.60
	27	4.0	70.85	0.60	1880	223.54	64.36
Turbojet mode	26	3.6	59.75	0.664	2188	222.54	71.94
	27	4.0	78.95	0.60	1880	223.54	71.72
	28	4.3	90.54	0.54	1616	224.54	71.56

	30	5.0	132.15	0.43	1197	226.51	71.83

According to aero-engine mass flow requirement from Table 1, the capture area of inlet is 4.8 m^2 at least to meet the flow requirement at Ma 5.0. At this capture area, the mass flow capture by the inlet is far more than engine requirement at the off-design point, as shown in Fig 1. For instance, at Ma 1.5, aero-engine needs 94 kg/s airflow while inlet capture flow ratio reaches about 300 kg/s, two third of the capture flow need to bypass the engine. If we aim at the engine requirement below Ma 3.6, the require capture area is 1.7 m^2. The require total pressure recovery at aerodynamic interface plane of the inlet is illustrated in Fig 2. It is between Military specification MIL-E-5008B and Aerospace Industries Association(AIA) specification. As we know, AIA specification is current level. Therefore, we need to further reduce the loss during the inlet and improve its total pressure recovery.

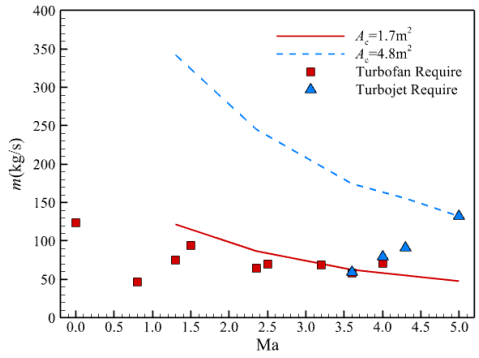

Fig 1. Inlet capture area requirement

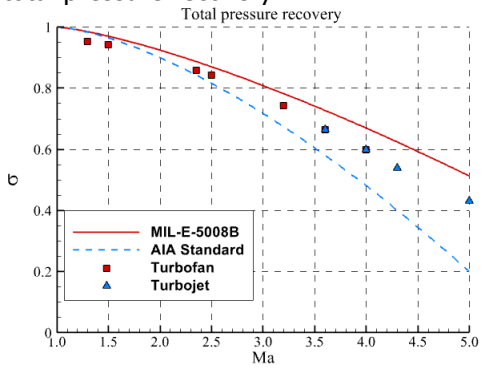

Fig 2. Inlet total pressure recovery requirement

Base on the inlet design requirement above, we design three different inlet schemes to meet the near term, mid-term and long term goal. The design point Mach number is Ma 2.5, Ma3.6 and Ma5.0, individually.

2.2. Baseline design point inlet geometry

The inlet with design point Ma 3.6 is selected as the baseline inlet. The design process of the baseline inlet is described in detail. The inlet consists of external compression ramps, internal compression and subsonic diffuser, which is shown in Fig. 3. The external compression ramps consists of a 10 deg curve ramp and 10 deg ramp at the design point. The width of the inlet is 1.24m and height 1.61m. Total compression ratio is 5.65 with internal compression ratio 2.65 at Ma 3.6. The deflection angle of cowl is 7 deg. There are six bleed slots at the shoulder of the inlet with 20mm in width. The centerline of the subsonic diffuser is set as rapid turning at the exit.

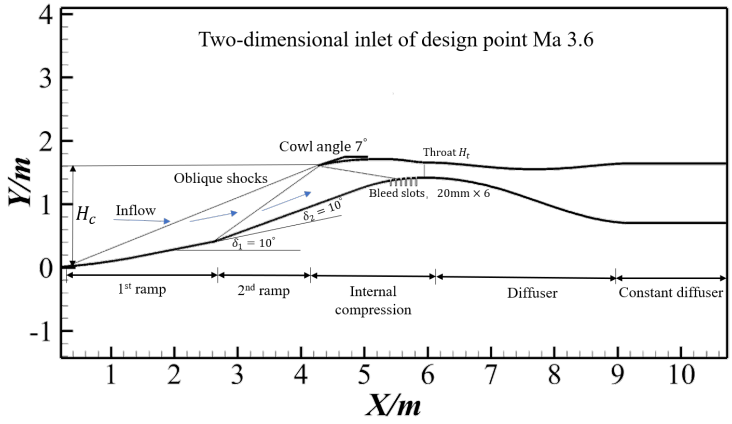

Fig 3. Two-dimensional inlet model at design point

2.3. Baseline off-design point inlet geometry

At the off-design point the inlet geometry is adjusted according to Fig 4. The first ramp angle is 10 deg until Ma 3.6 and then it increases to 13.5deg at Ma 5.0. The second ramp increases from 0 deg to 10

deg between Ma 0 and Ma 3.6 and then decreases to 7 deg. The internal compression ratio increases from 1.36 to 2.15 during Ma 1.5 and 3.6. The throat Mach number is designed to between Ma 1.2 and Ma 1.5, which is good to improve the performance of the inlet. The inlet geometry under Ma 3.6 and above Ma 3.6 are shown in Fig 5 and Fig 6, respectively.

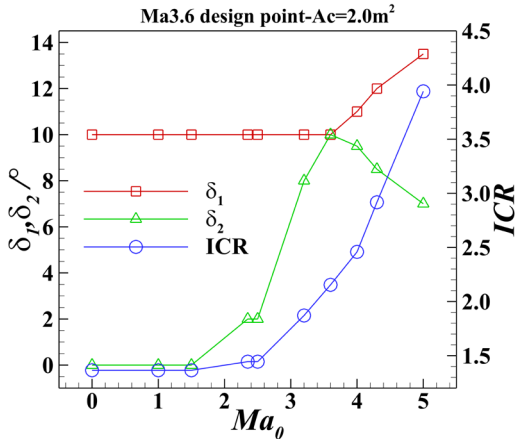

Fig 4. Variable geometry scheme

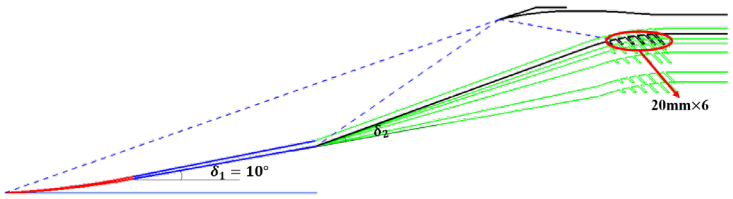

Fig 5. Variable inlet geometry under Ma 3.6

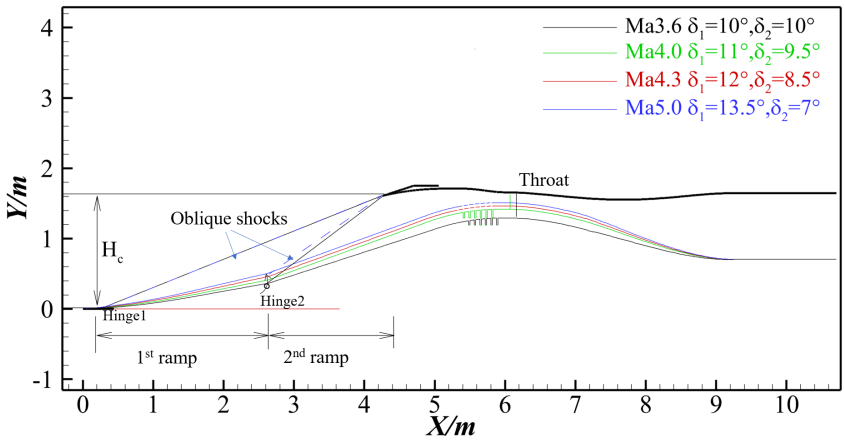

Fig 6. Variable inlet geometry above Ma 3.6

3. Numerical simulation method

The flow is modeled by the compressible steady RANS equations. The integral Cartesian form for an arbitrary control volume V with differential surface area dA as follows:

$$\frac{d}{dt}\int_V \boldsymbol{W}\mathrm{d}V + \oint\left[\boldsymbol{F}-\boldsymbol{G}\right]\cdot dA = \int_V \boldsymbol{H}\mathrm{d}V \tag{1}$$

where the vectors $\boldsymbol{W}$, $\boldsymbol{F}$ and $\boldsymbol{G}$ are defined as:

$$\boldsymbol{W}=\begin{Bmatrix}\rho\\ \rho u\\ \rho v\\ \rho w\\ \rho E\end{Bmatrix},\boldsymbol{F}=\begin{Bmatrix}\rho v\\ \rho vu+p\\ \rho vv+p\\ \rho vw+p\\ \rho vE+pv\end{Bmatrix},\boldsymbol{G}=\begin{Bmatrix}0\\ \tau_x\\ \tau_y\\ \tau_z\\ \tau_{ij}\cdot v_j+q\end{Bmatrix} \tag{2}$$

and the vector $\boldsymbol{H}$ contains source terms such as body forces and energy sources. Here ρ, v, E and p are the density, velocity, total energy per unit mass and pressure of the fluid, respectively. τ is the viscous stress tensor and q is the heat flux.

The inviscid flux vector $\boldsymbol{F}$ is evaluated by Roe flux-difference splitting scheme with the MUSCL interpolation method used to determinate the inviscid fluxes at the control surfaces. Temporal discretization of the coupled equations is accomplished by an implicit point Gauss-Seidel time-marching algorithm. The turbulence is modeled by two equations shear-stress transport (SST) $k-\omega$ model.

The near-wall modeling approach is adopted in the near-wall modeling in which the turbulence models are modified to enable the viscosity-affected region to be resolved with a mesh all the way to the wall, including the viscous sublayer. The air is modeled as an ideal gas with the specific heat ratio of $\gamma=1.4$ and the Sutherland's Law is used to account for the temperature variation of the molecular viscosity and the thermal conductivity.

The numerical simulations are performed by commercial solver. The inlet mesh and boundary conditions are shown in Fig 7. Total elements of structure mesh are about 260,000. Inflow boundary conditions are listed in Table 1. The simulations are considered converged when the outlet mass flow becomes stable and the residuals for mass, momentum and energy equations stop decreasing.

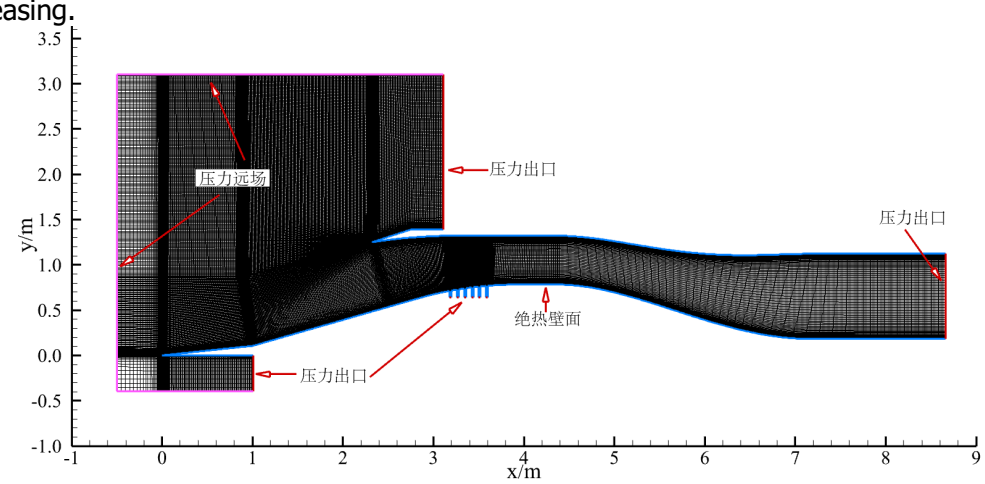

Fig 7. Inlet mesh and boundary conditions

4. Results

4.1. Design points capture mass flow comparison

To compare design point Mach number on the effect of inlet capture mass flow. We design three model at Ma 2.5, Ma 3.6 and Ma 5.0. The capture area of inlet is 2.0 m^2. The capture mass flow at different design points is shown in Fig 8.The results indicate that capture mass flow under Ma 3.6 meet the requirement. However, mass flow ratio of design point at Ma 3.6 is the best among these three inlet schemes. It increases linearly from 0.35 to 1.0 with inflow Mach number. The mass flow ratio of design point Ma 2.5 and Ma 5.0 decrease significantly at Ma 2.5.

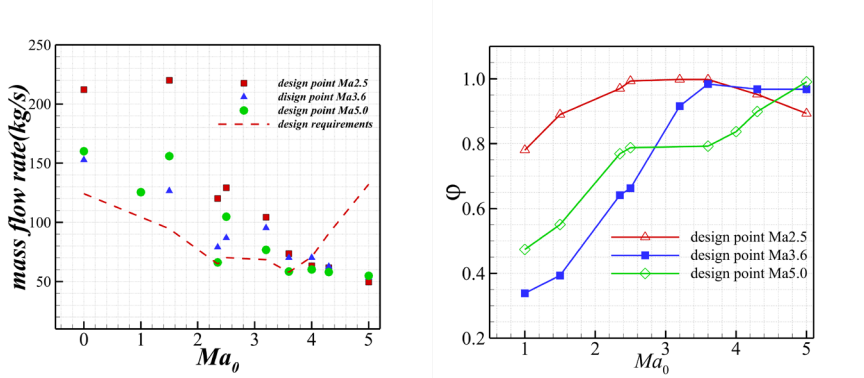

Fig 8. Inlet capture mass flow at different design points

Detail parameters of these three design points are shown in Table 2 to Table 4. The throat Mach number of design point Ma 2.5 and Ma 5.0 is wider than Ma 3.6, which is between Ma 1.2 and 1.5. This feature of throat Mach number within a small range at different inflow Mach number helps the improvement of inlet performance at a wide range.

Table 2. Design point Ma 2.5 parameters

Ma_0	m_i(kg/s)	Ma_t	φ_{inlet}	φ_{bleed}
1.5	219.90	1.05	0.6808	0.0375
2.35	120.24	1.41	0.9752	0.0066
2.5	129.25	1.25	0.9854	0.0171
3.6	73.59	1.82	0.9977	0.0092
4.3	61.64	1.81	0.9516	0.0354
5.0	49.62	1.66	0.8934	0.0504

Table 3. Design point Ma 3.6 parameters

Ma_0	m_i(kg/s)	Ma_t	φ_{inlet}	φ_{bleed}
1.5	126.95	0.87	0.3931	5.14
2.35	79.08	1.21	0.6414	3.16
2.5	86.89	1.34	0.6626	1.55
3.6	70.18	1.49	0.9517	6.07
4.3	62.70	1.39	0.9682	3.51
5.0	53.47	1.43	0.9627	9.20

Table 4. Design point Ma 5.0 parameters

Ma_0	m_i(kg/s)	Ma_t	φ_{inlet}	φ_{bleed}
1.5	155.86	1.07	0.4825	4.40
2.35	66.18	1.38	0.5367	1.04
2.5	104.68	1.25	0.7980	0.76
3.6	58.42	1.57	0.7920	7.46
4.3	57.98	1.55	0.8951	8.14
5.0	54.89	1.45	0.9882	10.68

4.2. Design points Ma3.6 inlet flow characteristics

According to the result above, design point Ma 3.6 inlet scheme is selected. Then we analyze the flow characteristics and performance of this inlet at different engine operation condition. We use backpressure to simulate the inlet operates at different engine operation conditions.

As shown in Fig 9, the terminal shock move from downstream to the upstream with backpressure increases from 0.7 to 0.88 times of inflow pressure. As inflow Mach number increase to Ma 1.5, a deattach shock is form at the external compression ramp and it moves to the tip of the compression ramp as the backpressure increases up to 3.3 times of inflow pressure. Meanwhile, a separation bubble appears at the inlet shoulder.

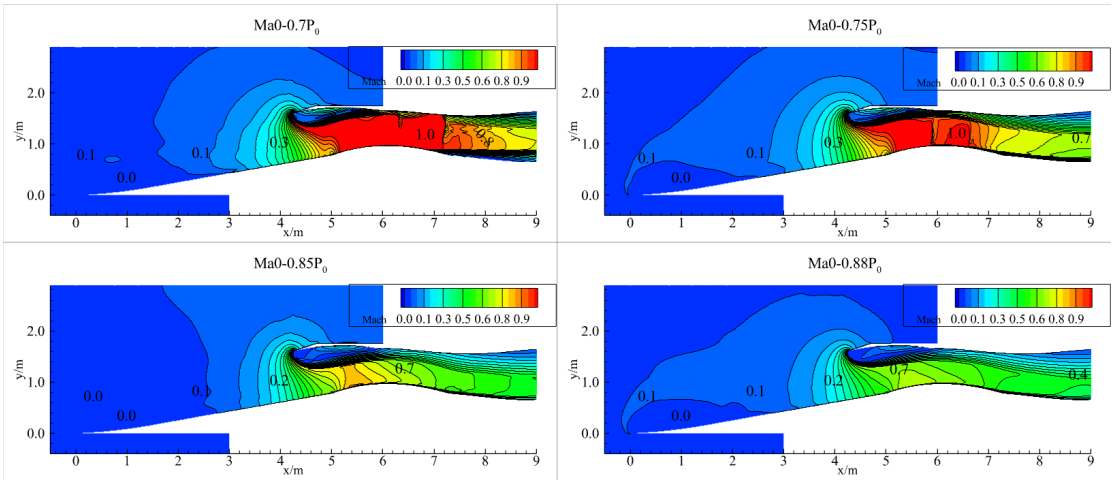

Fig 9. Flow characteristics of Ma 0 at different back pressure

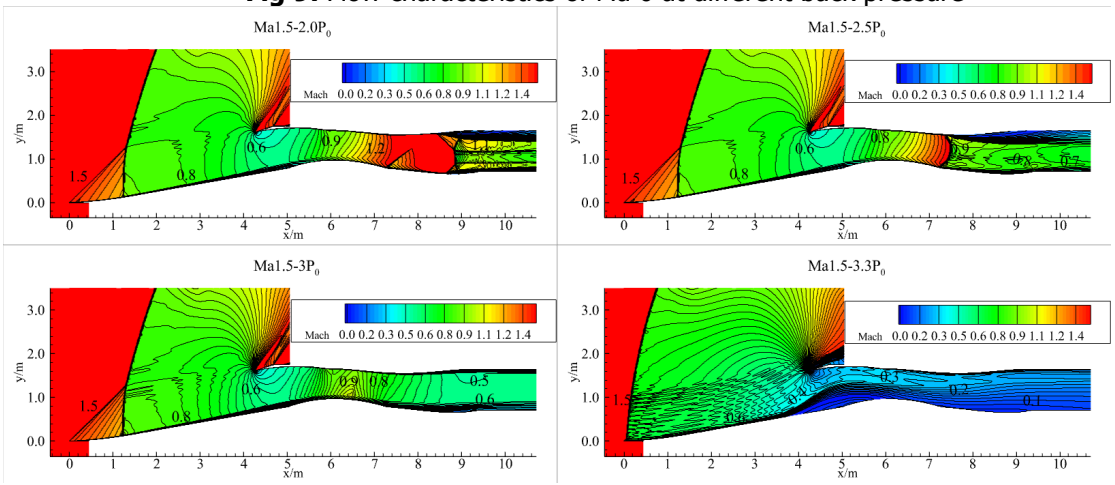

Fig 10. Flow characteristics of Ma 1.5 at different back pressure

As inflow increase further to Ma 2.5, the second compression ramp angle increase from 0 deg to 2 deg. As shown in Fig 11, there are two external shocks, the first one is curve compression shock and the second one is oblique shock. The supersonic flow is then compression by cowl reflection shock. As the back pressure increase the terminal shock move from downstream to the throat of the inlet. The inlet operates at critical state at backpressure 12 time of inflow static pressure. Th performance of inlet reaches its maximum 0.95.

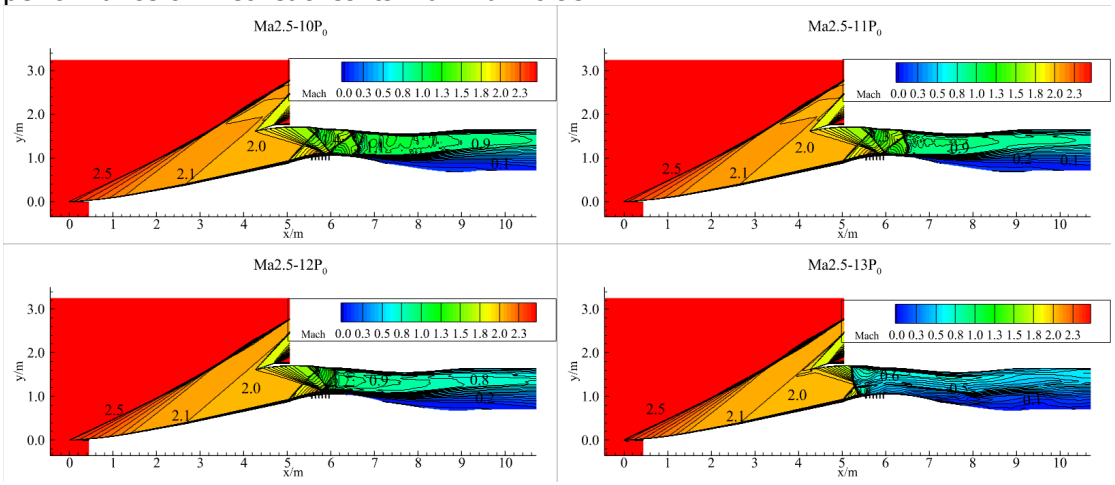

Fig 11. Flow characteristics of Ma 2.5 at different back pressure

As inflow increase further to Ma 3.6, the second compression ramp angle increase from 2 deg to 8 deg. The shock-on-lip condition is achieved at Ma 3.6, as illustrated in Fig 12. As the backpressure increases up to 52 time of inflow static pressure, the inlet operates at critical state with total

pressure recovery at aerodynamic interface plane 0.70.

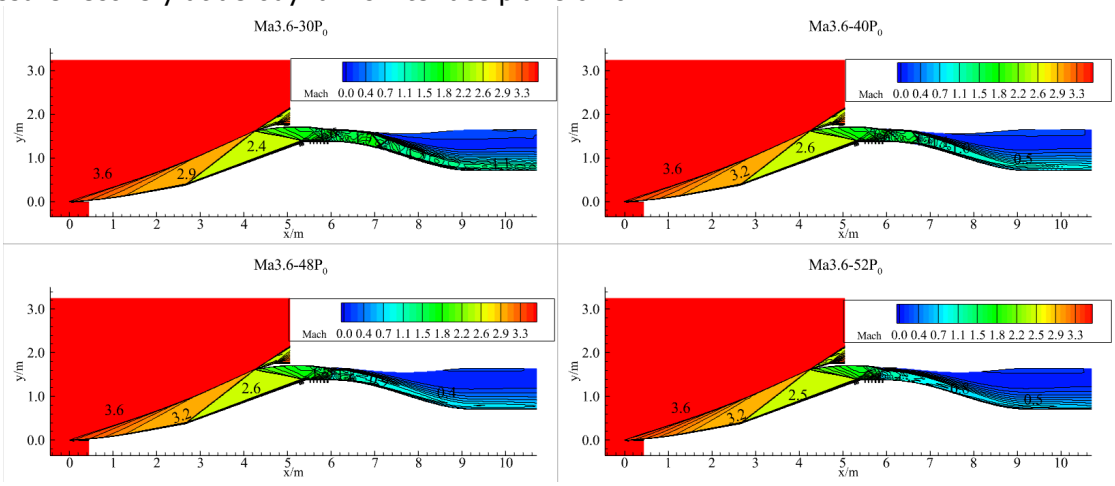

Fig 12. Flow characteristics of Ma 3.6 at different back pressure

As the design point is selected at Ma 3.6, at Ma 4.3 a shear layer would be digested into the inlet. Therefor, we increase the angle of the first ramp from 10 deg to 12 deg. As shown in Fig 13, shock-on-lip condition is also achieved at Ma 4.3. The throat Mach is about 1.5. With the inlet shoulder bleed, the shock/boundary layer interaction is weaken this improve the performance of the inlet. As the backpressure of the inlet increases up to 110 time of inflow pressure, the inlet operates at critical state and the total pressure recovery is 0.54.

As inflow increase further to Ma 5.0, the first ramp angle increase from 12 deg to 13 deg, with internal compression ratio 3.26. To reduce the boundary layer from the inlet cowl, we add two more bleed slots at the cowl side of the throat section, as shown in Fig 14.

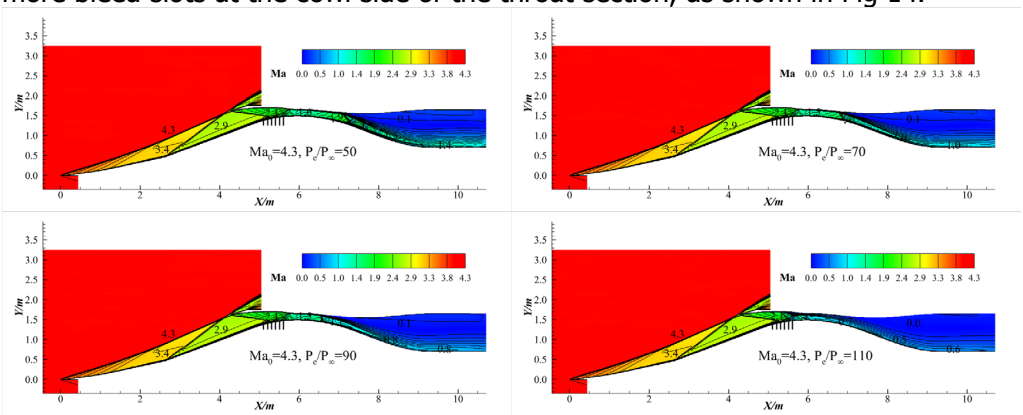

Fig 13. Flow characteristics of Ma 4.3 at different back pressure

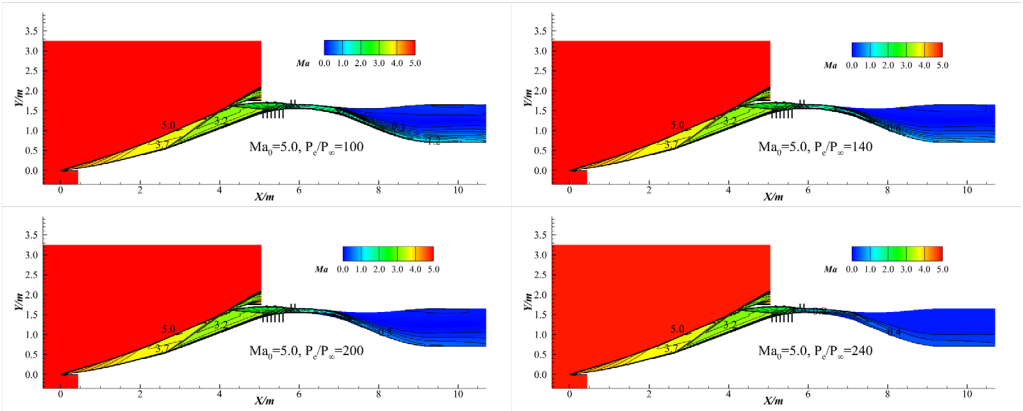

Fig 14. Flow characteristics of Ma 5.0 at different back pressure

According to the flow characteristics analysis in previous, the total pressure recovery, mass flow ratio and Mach number at AIP are summarized in Fig 15. As shown in Fig 15(a), total pressure recovery increases with backpressure due to the terminal shock moves from downstream to the upstream of the

inlet. As the terminal shock moves to the throat, the total pressure recovery reaches its maximum. Then the mass flow ratio and total pressure recovery decrease with the terminal shock moves to the upstream of the inlet cowl. Mass flow spillage increases downstream the terminal shock, the flow into the inlet reduces. The match point mass flow and total pressure recovery are summarized in Fig 15(b), the results indicate that the inlet performance meet the requirement of the inlet between Ma 0 and Ma 3.6. The detail results of the inlet at the match point are listed in Table 5.

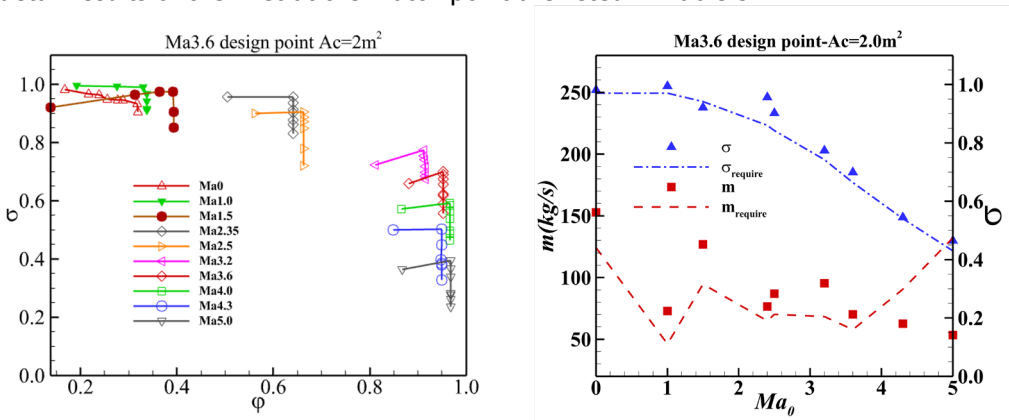

Fig 15. Design point Ma 3.6 inlet scheme inlet performance

Table 5. Design point Ma 3.6 inlet scheme match point performance

Ma_0	m(kg/s)	Ma_t	φ_{inlet}	σ_e	Ma_e
0.0	152.83	1.22	0.3188	0.9813	0.59
1.0	72.83	0.87	0.3382	0.9945	0.25
1.5	126.95	0.87	0.3931	0.9209	0.38
2.4	76.57	1.21	0.6414	0.9562	0.42
2.5	86.89	1.34	0.6626	0.9019	0.53
3.2	95.33	1.45	0.9231	0.7736	0.48
3.6	70.18	1.49	0.9517	0.6989	0.50
4.3	62.69	1.39	0.9680	0.5445	0.37
5.0	53.47	1.43	0.9627	0.4650	0.20

5. Conclusion

In order to meet the mass flow requirements of the new concept aero-engine within a wide range Mach number, we design a variable geometry two-dimension inlet. The variable geometry scheme and flow characteristics of the inlet are investigated. The results indicated that:

1. This paper presents the design of a mixed compression inlet with a combination of curved isentropic compression and oblique compression. The throat Mach number is controlled to be around Ma 1.2-1.5 at different inflow conditions.
2. We compare three different design Mach number(Ma 2.5, Ma 3.6 and Ma 5.0) inlet scheme at the same capture area. It was found that the flow characteristics of design point Ma3.6 inlet scheme is the best among three inlet schemes.
3.The mass flow and total pressure recovery of the two-dimensional variable geometry inlet meet the requirement of aero-engine below Ma 3.6, the total pressure recovery at Ma3.6 reaches about 0.70.

Acknowledgement

This research was funded by the National Natural Science Foundation of China (12302299), the Science Center for Gas Turbine Project (P2022-B-I-004-001), and the Scramjet Technology Key Laboratory Foundation (2023-JCJQ-LB-018-07).

References

[1] Van Wie D M,Kwok F T,Walsh R F.Starting characteristics of supersonic inlet[R].AIAA 96-2914,1996.
[2] Seddon J, GoldSmith E L, Intake aero dynamics[M].2nd ed.Oxford:Blackwell Science Ltd,1999.
[3] Yu H, Zhang Y, Chen L, et al. Characteristics of combined-cycle inlet during mode transition in off-design state [J] . AIAA Journal, 2023 61(6), 2601-2611.
[4] Tan H, Guo R.Wind tunnel tests of hypersonic inlets for ramjet modules of ramjet-scramjet combined engine[J]. ACTA AERONAUTICAET ASTRONAUTICA SINICA, 2007, 28(4): 783-790. (in Chinese)
[5] Li Q, Gui F. Design and experimental development overview of foreign TBCC inlet technology [J]. Gas Turbine Experiment and Research, 2019, 32(03):58-62.(in Chinese)
[6] Wang J, Mu H, Gong C. Optimal design of wide-speed range two-dimensional inlet with free configuration[J]. Journal of Rocket Propulsion,2022,48(06):92-100. (in Chinese)
[7] Zhu W, Wang X, Hua Z. Design and experimental research of Mach number range 0—4 2D mixed parallel-type curved compression inlet[J]. Journal of Aerospace Power,2023,38(09):2271-2278. DOI:10.13224/j.cnki.jasp.20220449. (in Chinese)
[8] Taguchi H, Futamura H, Shimodaira K,et al.Design Study on Hypersonic Engine Components for TBCC Space Planes[C]//Aiaa International Space Planes & Hypersonic Systems & Technologies.2011. DOI:10.2514/6.2003-7006.
[9] Sanders B W, Weir L J.Aerodynamic Design of a Dual-Flow Mach 7 Hypersonic Inlet System for a Turbine-Based Combined-Cycle Hypersonic Propulsion System[R]. 2008. DOI:http://ntrs.nasa.gov/search.jsp?R=20080030791.
[10] Liu Y, Jin Z, Zhang K. Parameters analysis of adaptive pressure relief slot in hypersonic inlet[J]. Journal of Aerospace Power, 2013(6):9.DOI:10.3969/j.issn.1673-1999.2014.07.010. (in Chinese)
[11] Yuan H, Liang D. Effect of suction on starting of hypersonic inlet[J]. Journal of Propulsion Technology,2006(06):525-528.DOI:10.13675/j.cnki.tjjs.2006.06.011. (in Chinese)
[12] Chen H, Huang H, Tan H. Effects of configuration and slot angle of the bleed system on the performance of hypersonic inlet[J]．Physics of Gases,2023,8(2):24-31. (in Chinese)